

1 ***Supporting Information Appendix***

2 **Larger but younger fish when growth compensates for higher**
3 **mortality in heated ecosystem**

4
5 Max Lindmark^{a,b,1}, Malin Karlsson^a, Anna Gårdmark^c

6
7 ^a Swedish University of Agricultural Sciences, Department of Aquatic Resources, Institute of
8 Coastal Research, Skolgatan 6, 742 42 Öregrund, Sweden

9 ^b Swedish University of Agricultural Sciences, Department of Aquatic Resources, Institute of
10 Marine Research, Turistgatan 5, 453 30 Lysekil , Sweden

11 ^c Swedish University of Agricultural Sciences, Department of Aquatic Resources, Skolgatan 6,
12 SE-742 42 Öregrund, Sweden

13
14 ¹ Author to whom correspondence should be addressed. Current address:

15 Max Lindmark, Swedish University of Agricultural Sciences, Department of Aquatic
16 Resources, Institute of Marine Research, Turistgatan 5, 453 30 Lysekil , Sweden, Tel.:
17 +46(0)104784137, email: max.lindmark@slu.se

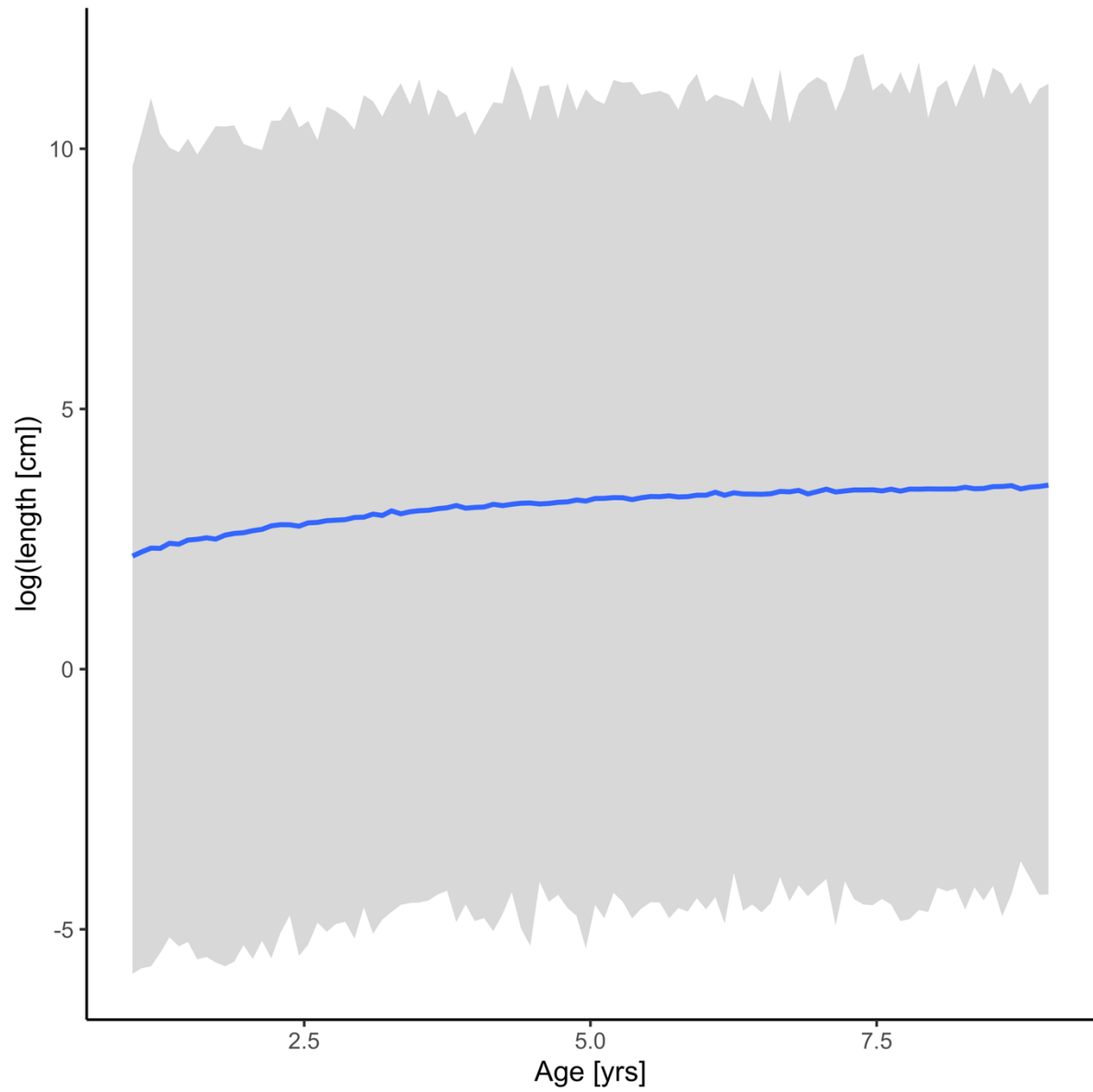
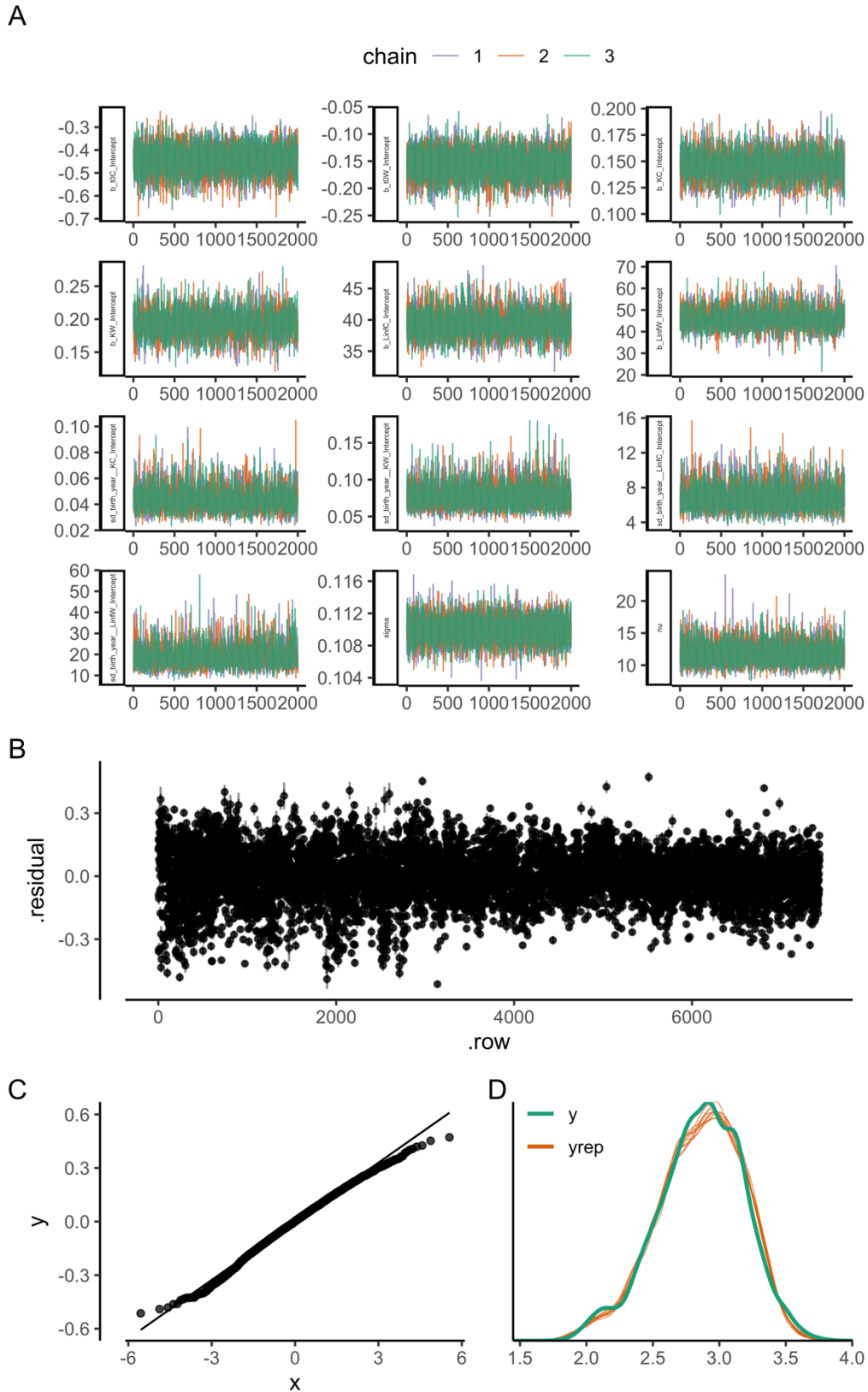


Fig. S1. Prior predictive distribution for the von Bertalanffy growth equation (posterior draws from the prior only, ignoring the likelihood). The solid line is the median and the shaded area is the 95% credible intervals.

Table S1. Comparison of von Bertalanffy growth models with different combinations of shared and area-specific parameters (ordered by difference in expected log pointwise density (elpd) from the best model). Note that in all models, $L_{\infty j}$ and K_j vary among cohorts.

Model Name	Model structure	elpd_diff
M1	Area-specific $L_{\infty j}$, K_j and t_0	0
M4	Area-specific $L_{\infty j}$ and K_j , common t_0	-9
M2	Area-specific K_j , common t_0 and $L_{\infty j}$	-111
M3	Area-specific t_0 and $L_{\infty j}$, common K_j	-150.5
M7	Area-specific $L_{\infty j}$, common K_j and t_0	-157.7
M6	Area-specific K_j , common t_0 and $L_{\infty j}$	-173.9
M5	Area-specific t_0 , common K_j and $L_{\infty j}$	-1337.5
M8	Common t_0 , K_j and $L_{\infty j}$	-2153.8



48

49 Fig. S2. The best model of the von Bertalanffy growth equation: (A) traceplot to illustrate chain
 50 convergence for key (population-level) parameters, (B) residuals, (C) QQ-plot and (D)
 51 posterior predictive check (D).

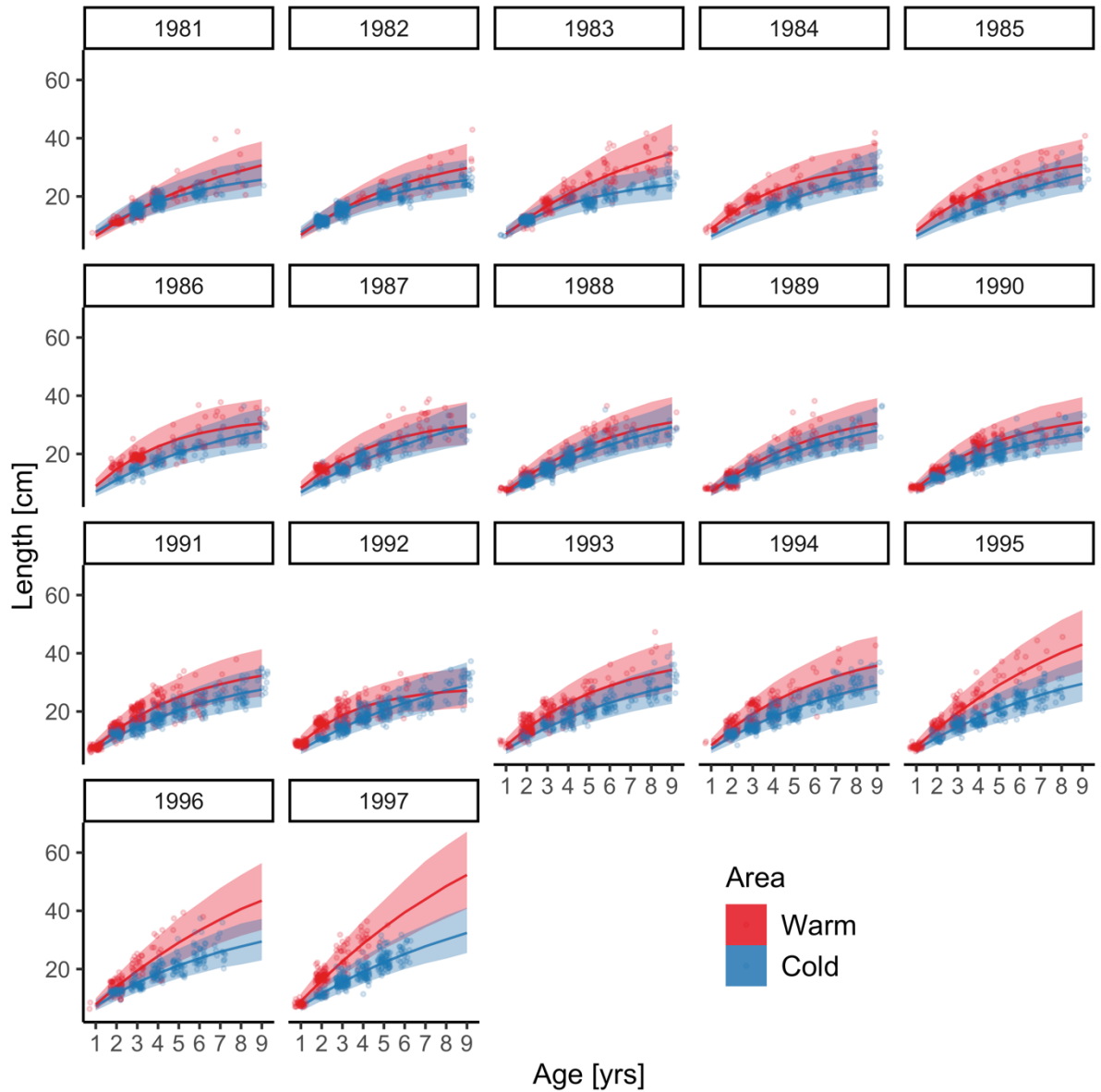


Fig. S3. Cohort-specific predictions from the best von Bertalanffy model (i.e., with cohort-varying L_{∞} and K). Points correspond to data, solid lines correspond to the median of the posterior prediction from the model and the shaded area corresponds to the 95% credible interval.

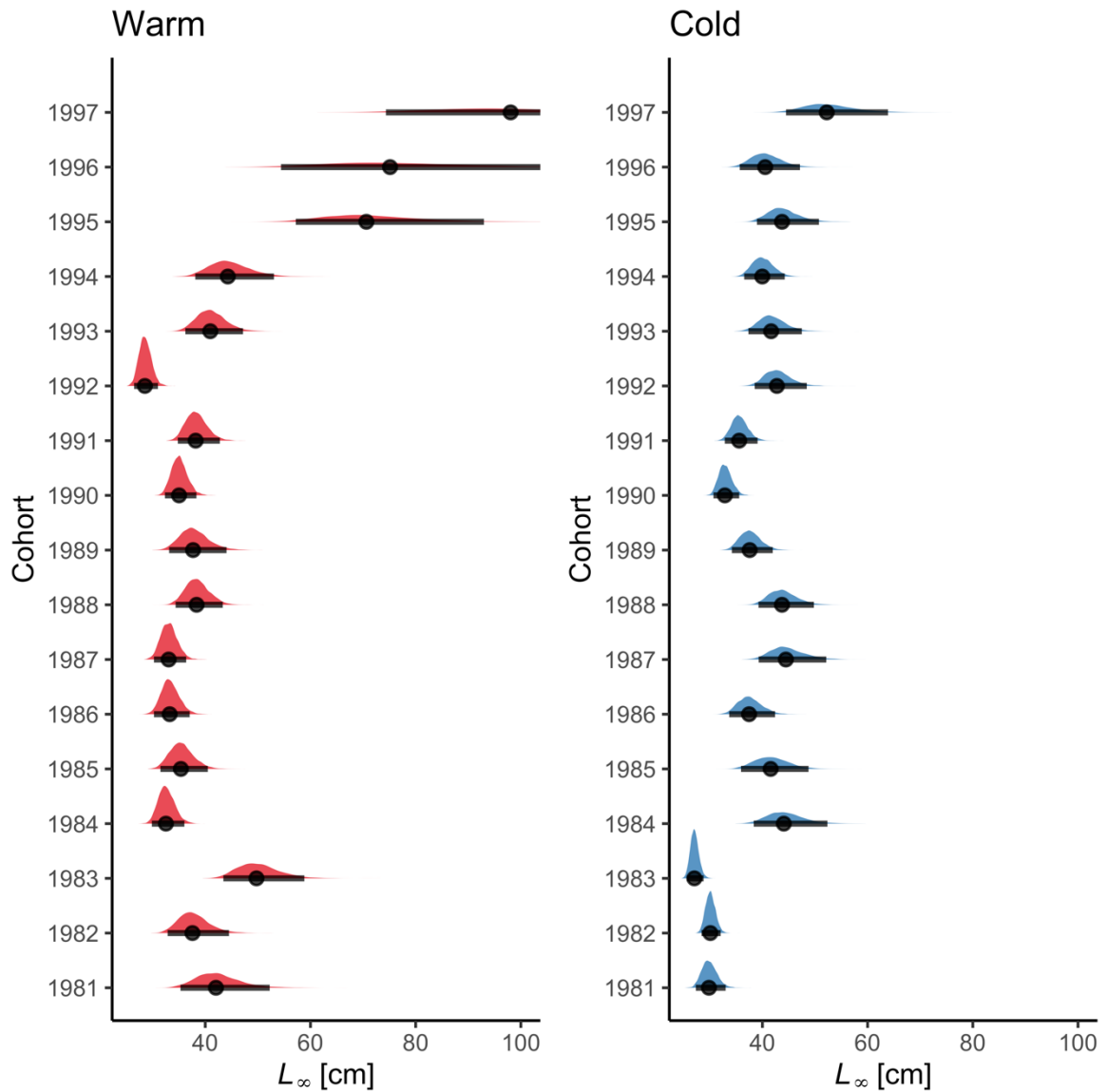


Fig. S4. Posterior distributions of the cohort-varying L_{∞} parameter in the best von Bertalanffy growth model. Points correspond to the median and the horizontal lines correspond to the 95% credible interval. Note that the distributions of L_{∞} in the warm areas extend beyond the x-axis for cohorts 1995–1997 (also evident in Fig. S3). The range of the x-axis was set to be wide enough to include the posterior medians of the larger estimates but narrow enough to allow for comparison between the other cohorts and areas.

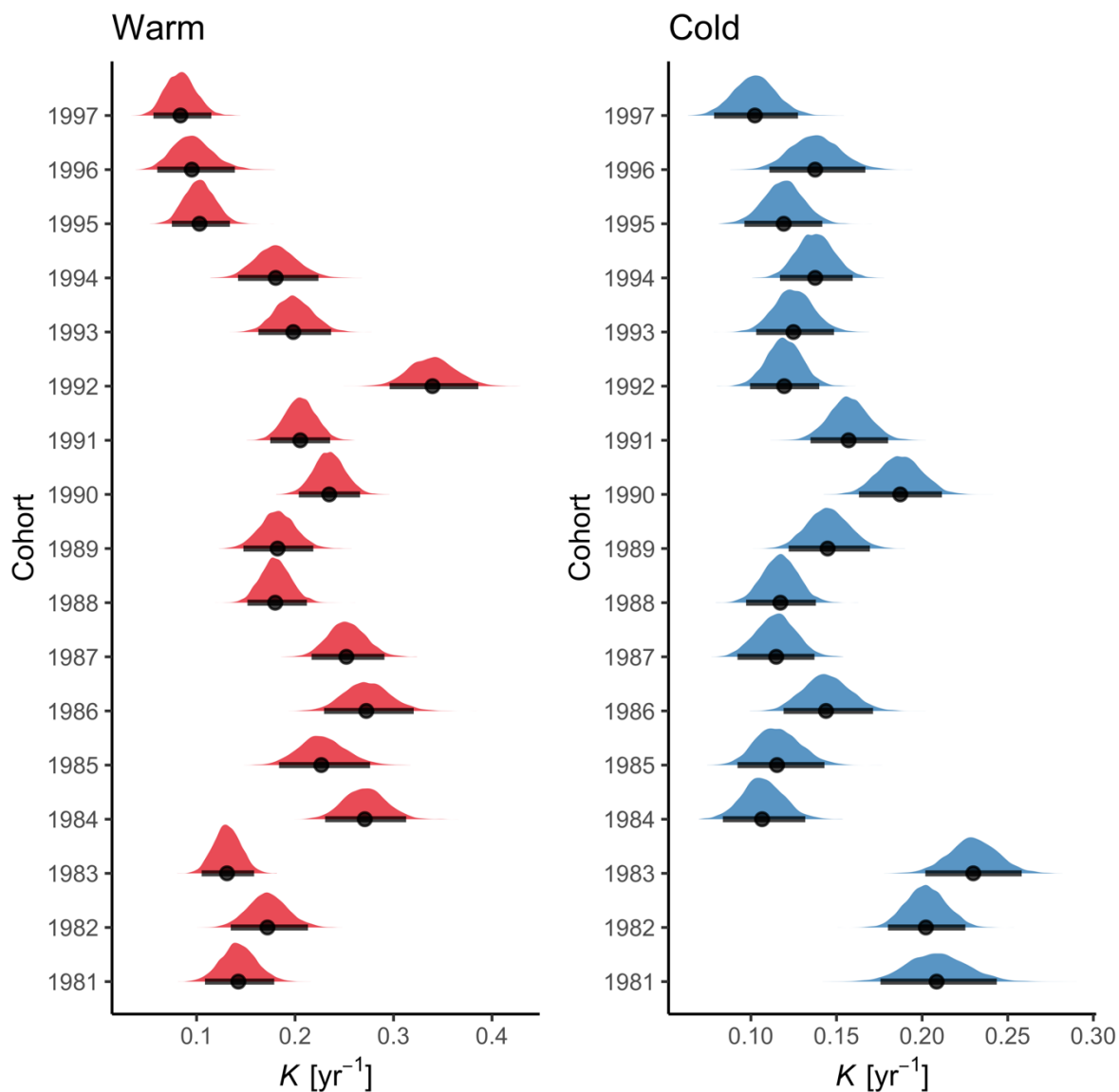
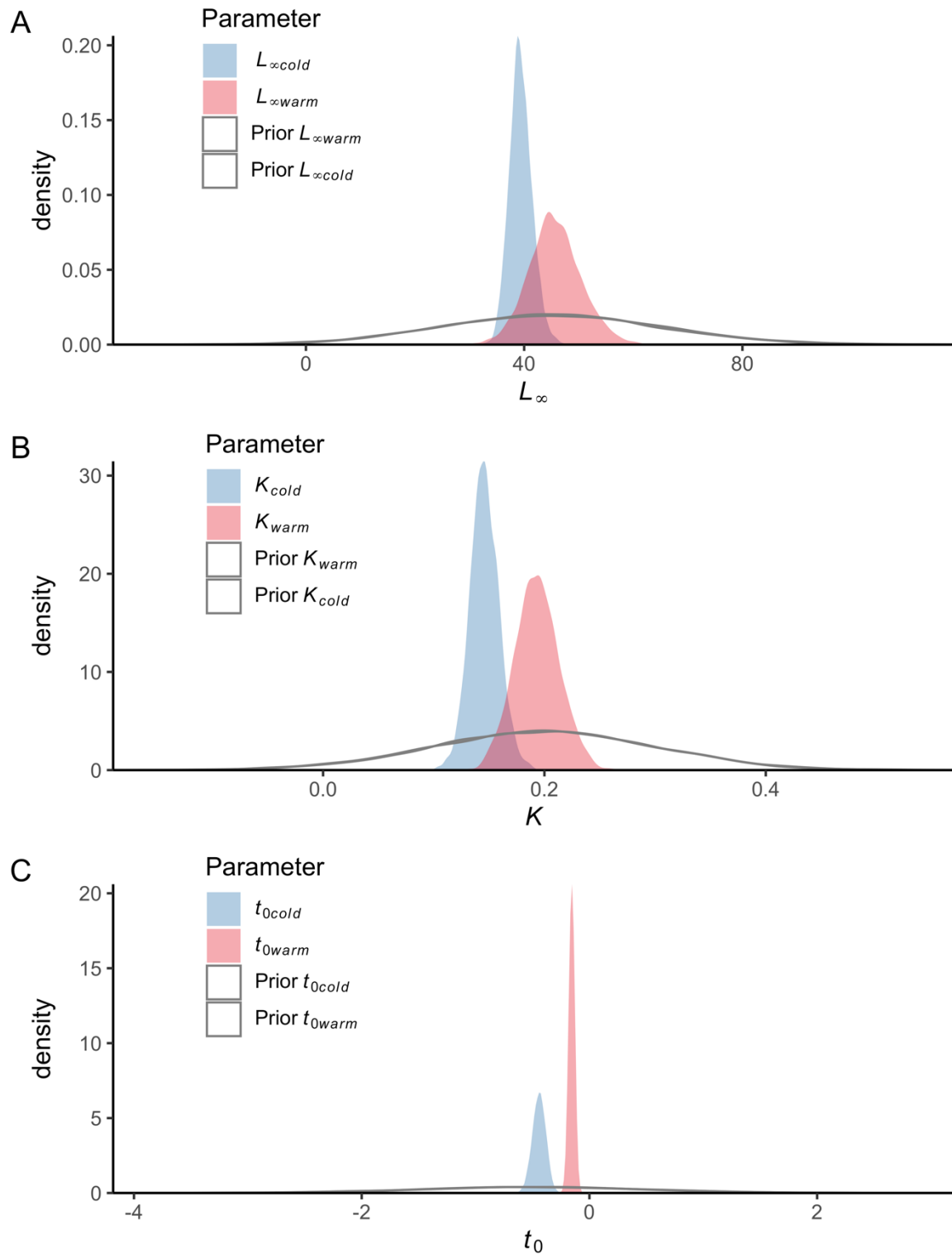


Fig. S5. Posterior distributions of the cohort-varying K parameter in the von Bertalanffy model. Points correspond to the median and the horizontal lines correspond to the 95% credible interval.



79

80 Fig. S6. Prior vs posterior distributions for parameters L_{∞} (A), K (B) and t_0 (C) in the best
 81 model of the von Bertalanffy growth equation.

82

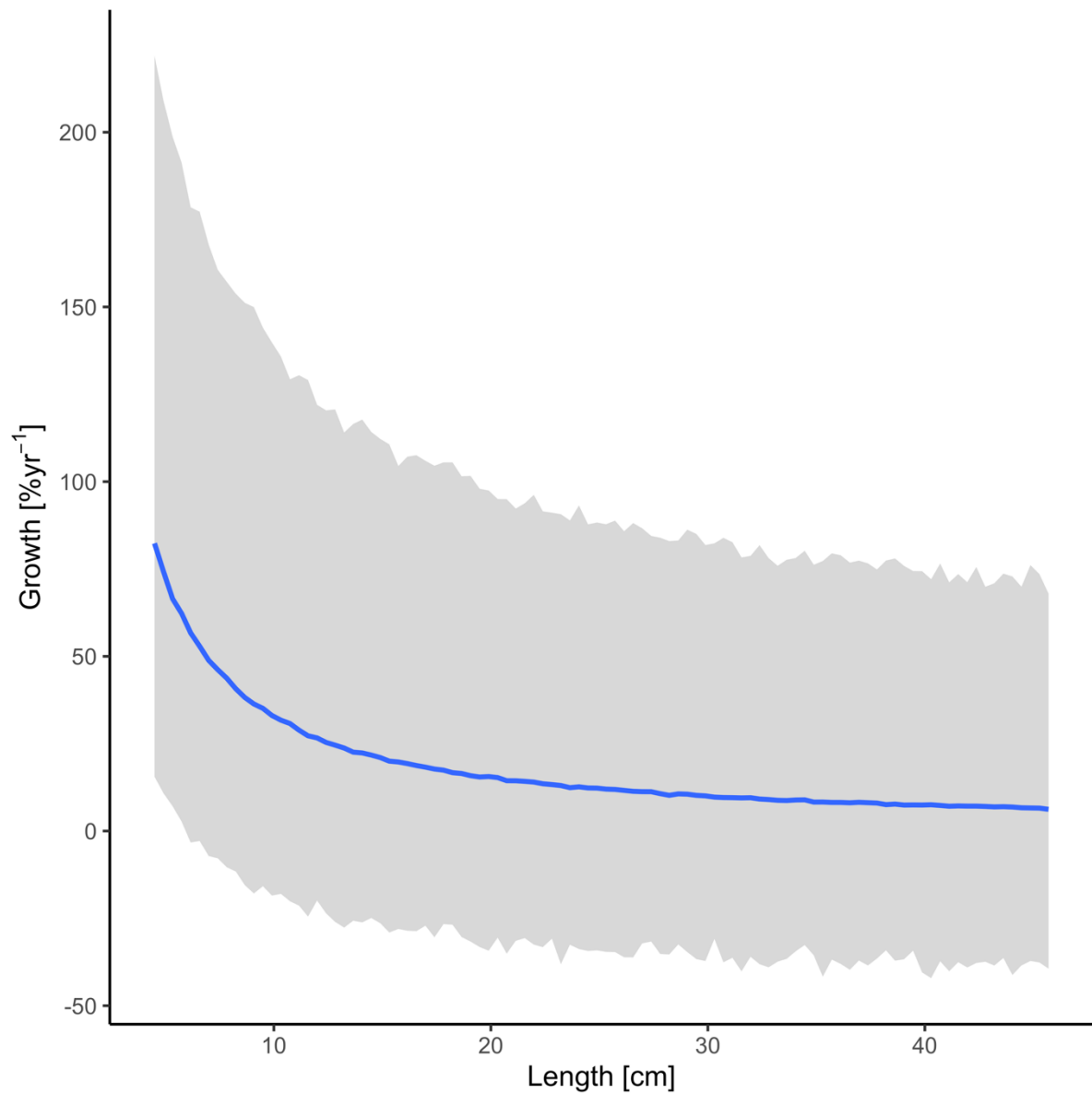
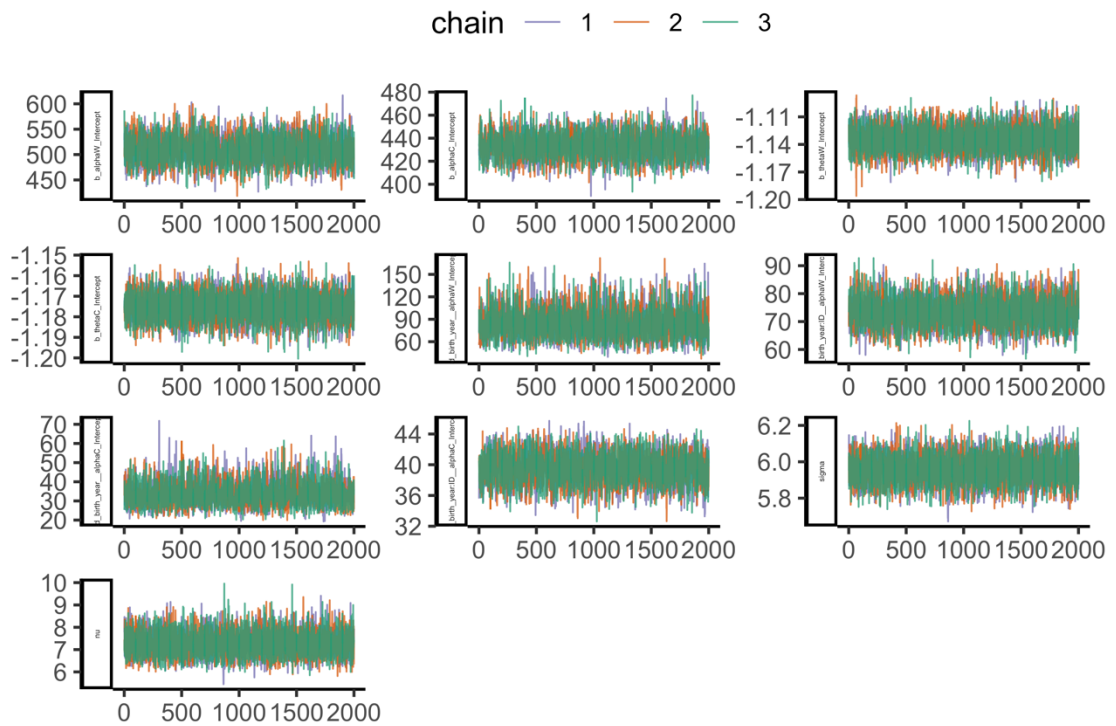


Fig. S7. Prior predictive distribution for the allometric growth model (posterior draws from the prior only, ignoring the likelihood). The solid line is the median and the shaded area is the 95% credible intervals.

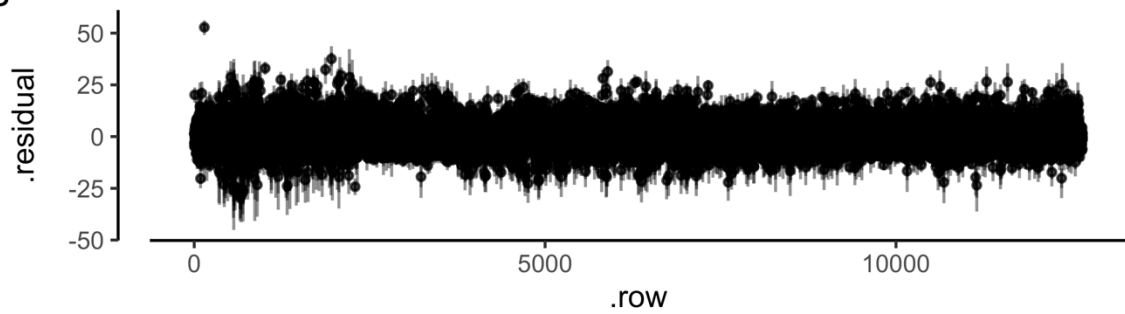
Table S2. Comparison of allometric growth models with common or unique θ -parameter (exponent in the allometric growth model), ordered by difference in expected log pointwise density (elpd) from the best model.

Model Name	Model structure	elpd_diff
M1	Intercept ($\alpha_{j[i],k[i]}$) varying across individuals within cohorts, fixed, area-specific slope (θ_R, θ_H)	0
M2	Intercept ($\alpha_{j[i],k[i]}$) varying across individuals within cohorts, “fixed” common slope (θ)	-2.7

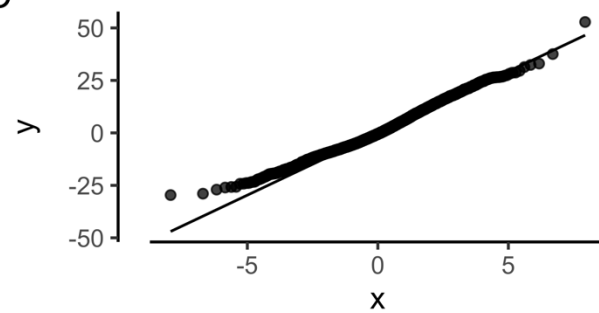
A



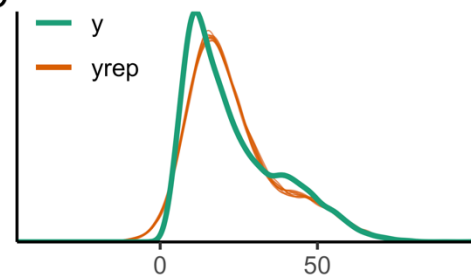
B



C



D



109

110 Fig. S8. The best allometric growth model: (A) traceplot to illustrate chain convergence for
 111 key (population-level) parameters, (B) residuals, (C) QQ-plot and (D) posterior predictive
 112 check (D).

113

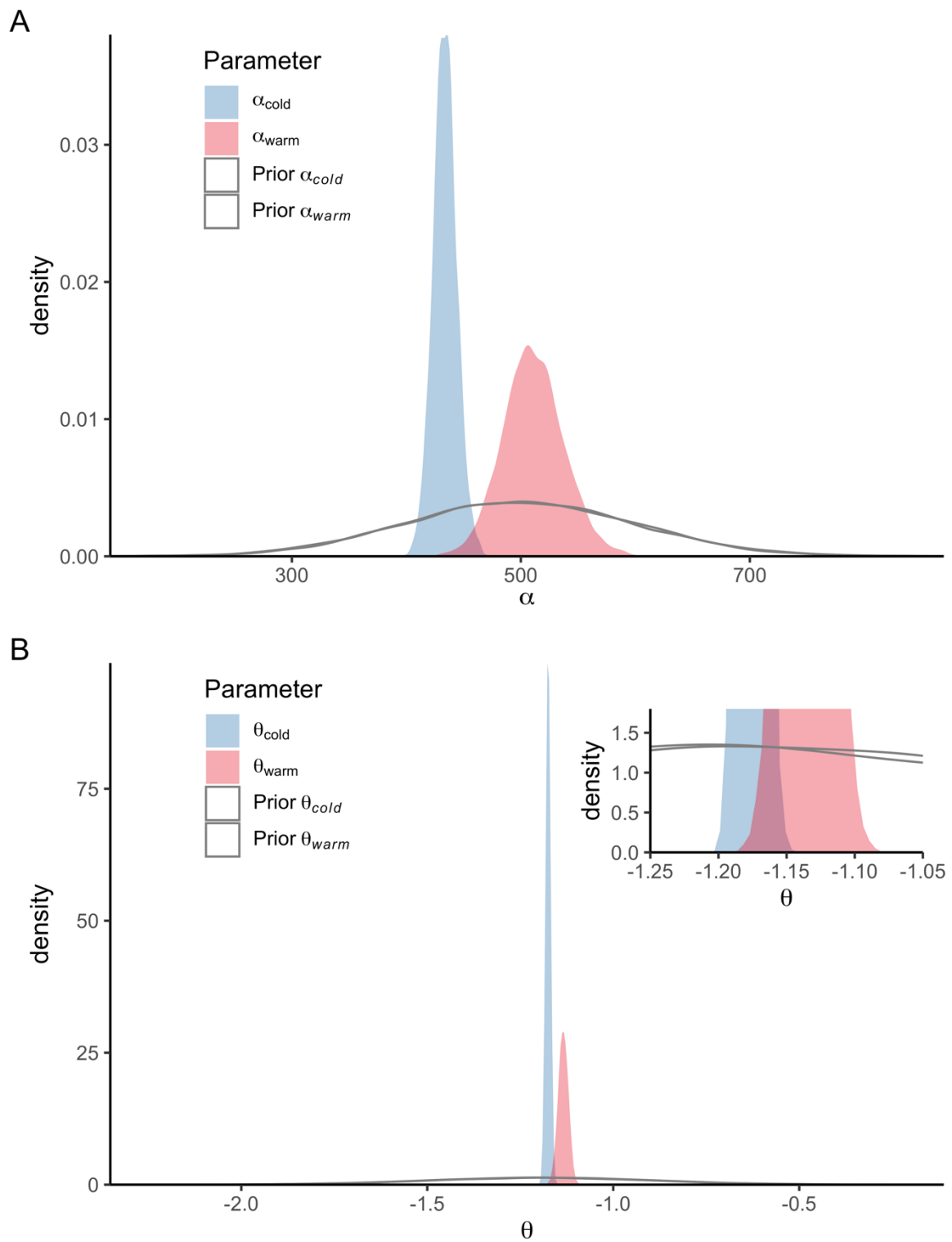


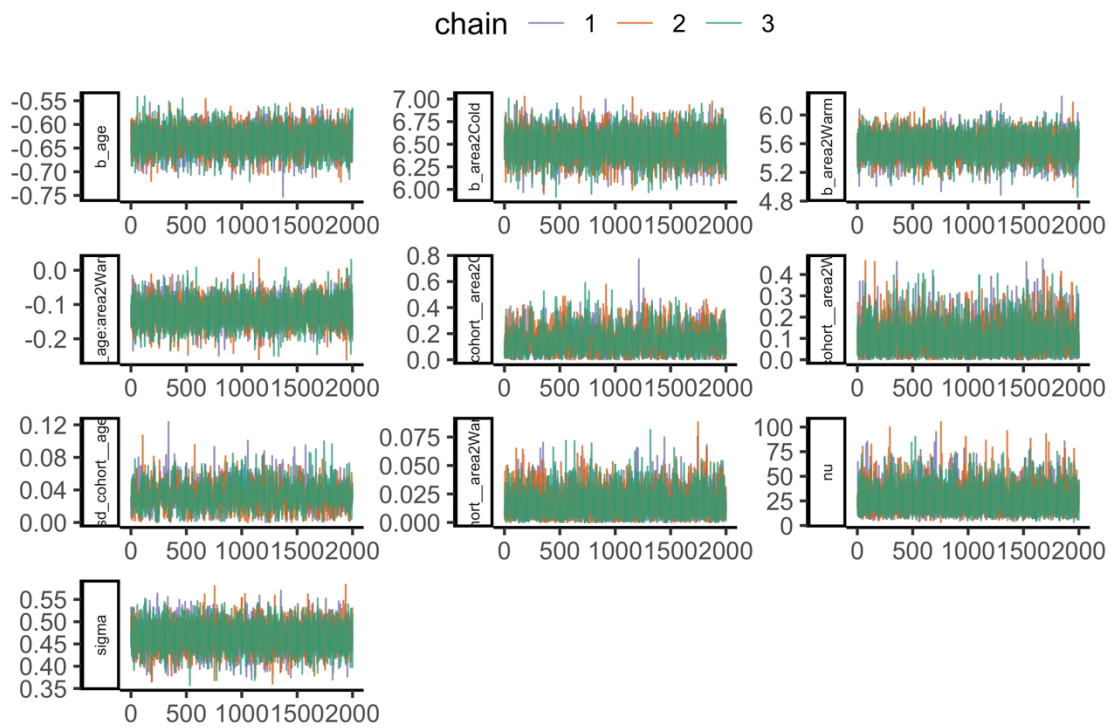
Fig. S9. Prior vs posterior distributions for parameters α (A) and θ (B) in the best allometric growth model (inset in panel (B) is a zoomed-in version to better visualize the priors in the range of the posteriors).

119 *Table S3 Comparison of catch-curves models with “fixed” or random (i.e., varying by*
 120 *cohort) slopes. Models ordered by difference in expected log pointwise density (elpd) from*
 121 *the best model.*

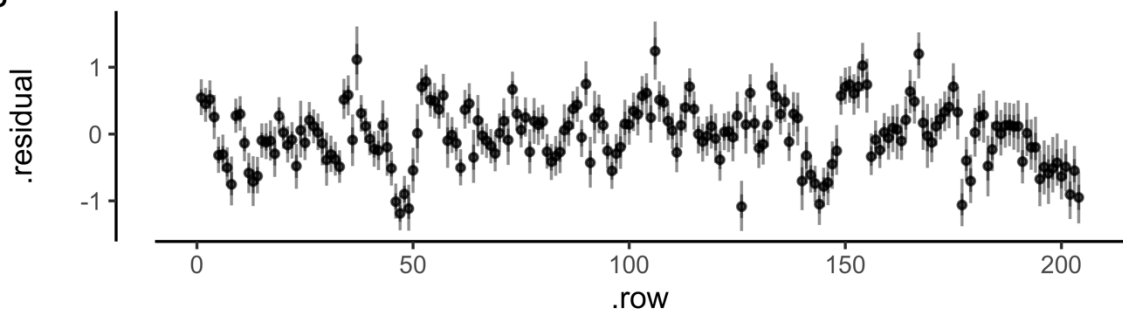
Model Name	Model structure	elpd_diff
M1	Area-specific and cohort varying α_j , area-specific θ	0
M2	Area-specific and cohort varying α_j and θ_j	-1.2

122

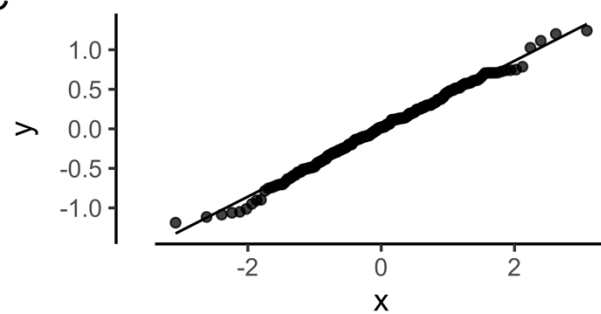
A



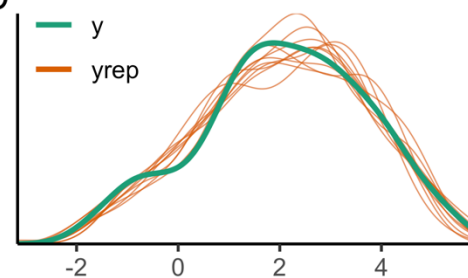
B



C



D



123

124 Fig. S10. The best catch curve model: (A) traceplot to illustrate chain convergence for key
 125 (population-level) parameters, (B) residuals, (C) QQ-plot and (D) posterior predictive check
 126 (D).

127

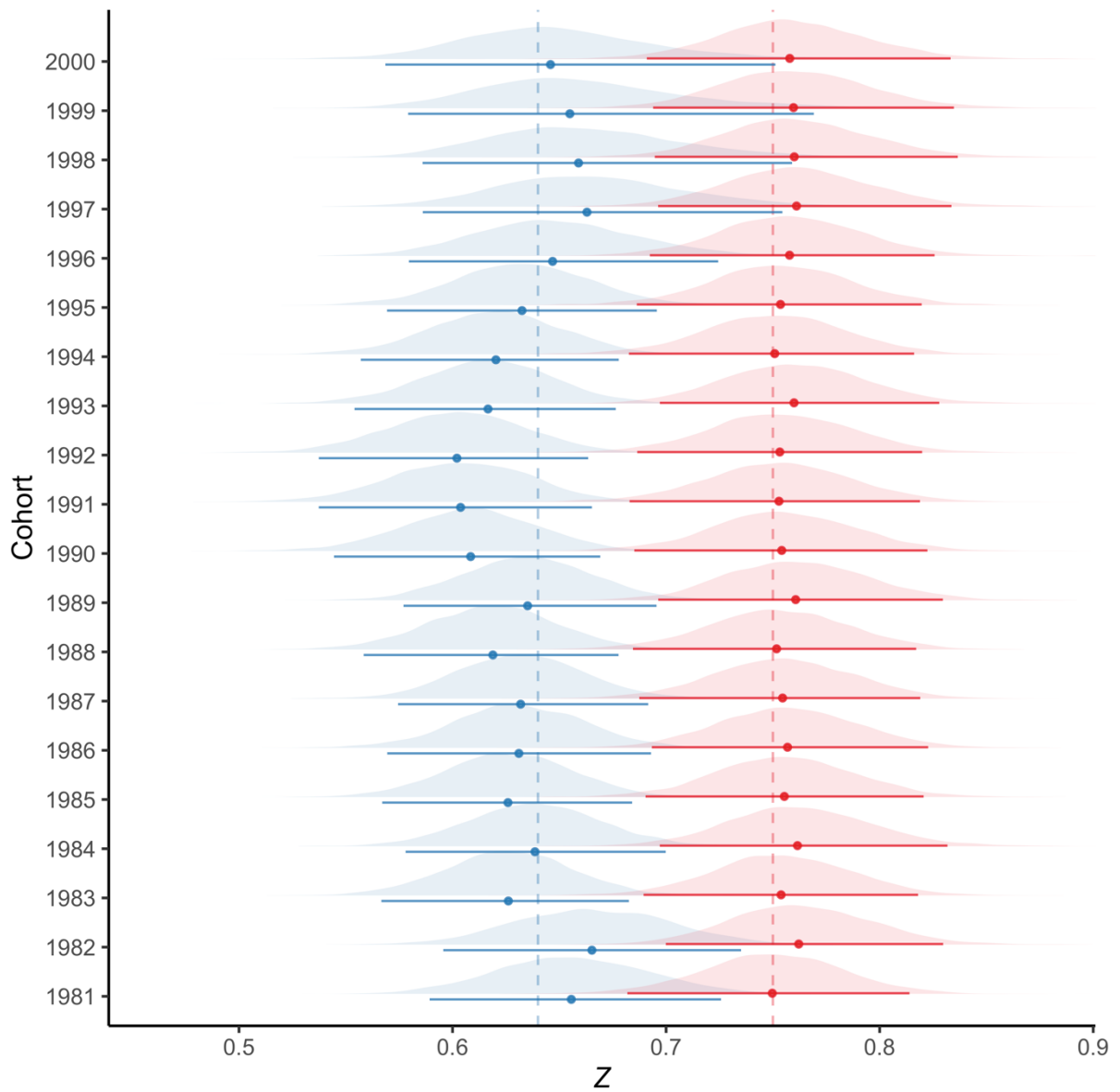


Fig. S11. Posterior distributions of the cohort-varying slopes in the best catch curve model, where Z , the mortality rate, is the negative of the slope of natural log of catch per unit effort (CPUE) as a function of age. Points correspond to the median and the vertical lines correspond to the 95% credible interval.